





Giant retardation effect in electron-electron interaction

Zhimin Hu ^{1,*}, Gang Xiong,^{2,3} Zhencen He,^{1,2} Zhihao Yang,¹ Naoki Numadate,⁴ Chengwu Huang,³ Jiamin Yang,³ Ke Yao,^{2,†} Baoren Wei,² Yaming Zou,² Chensheng Wu ⁵, Yulong Ma ⁵, Yong Wu,⁵ Xiang Gao ^{5,6,‡} and Nobuyuki Nakamura⁴

¹Key Laboratory of Radiation Physics and Technology of Ministry of Education, Institute of Nuclear Science and Technology, Sichuan University, Chengdu 610064, China

²Key Laboratory of Nuclear Physics and Ion-Beam Application (MOE), Institute of Modern Physics, Fudan University, Shanghai 200433, China

³Laser Fusion Research Center, China Academy of Engineering Physics, Mianyang 621900, China

⁴Institute for Laser Science, The University of Electro-Communications, Tokyo 182-8585, Japan

⁵Institute for Applied Physics and Computational Mathematics, Beijing 100088, China

⁶Beijing Computational Science Research Center, Beijing 1000193, China



(Received 9 February 2022; accepted 16 March 2022; published 29 March 2022)

In electron-electron interactions in electromagnetic systems, retardation in the exchange of a virtual photon is essentially important as the first-order quantum electrodynamics correction. However, the retardation effect is generally so small that it is buried in unretarded electric and magnetic interactions and thus has yet to be directly probed. Here, we present a giant contribution of the retardation effect in an electron-electron interaction via observing strong electric-dipole-allowed radiative transition rates. The relative transition rates are obtained for two dominant radiative transitions from the $1s2s^22p_{1/2}2p_{3/2}$ inner-shell excited state of boronlike tungsten and bismuth ions to $1s^22s^22p_{1/2}$ and $1s^22s^22p_{3/2}$, and it was found that the transition rate ratio between the two transitions is affected by the retardation effect up to more than 100%.

DOI: [10.1103/PhysRevA.105.L030801](https://doi.org/10.1103/PhysRevA.105.L030801)

Retardation effects are of essence in electromagnetic systems. They have attracted much interest in recent years in different physics fields, e.g., the nondipole effects in electron-photon interactions [1–6], as well as the Casimir effects which are retardation effects between induced dipole moments [7–12]. The electron-electron interaction is one of the most important electromagnetic interactions in atomic and molecular systems that constitute the matter world. The retardation effects of the electron-electron interaction are included in the so-called Breit interaction [13,14], which is a composite interaction caused by the first-order corrections to the Coulomb interaction due to the exchange of a virtual photon between interacting electrons, based on quantum electrodynamic (QED) theory [15–17].

The Breit interaction contains the unretarded magnetic current-current interaction (i.e., the Gaunt interaction) due to the motion of electrons [18], and retardation in the exchange of the virtual photon, which travels with the speed of light c . The retardation effects are the most crucial relativistic effects as the magnetic effects can be considered as a motion effect of the electron even in the nonrelativistic theory. These effects are generally small in atomic bound states, especially for the retardation effect, which is usually less than 10% of the Gaunt interaction and can even be smaller than other high-order QED effects (e.g., the

Lamb shifts) in heavy ions [19–21]. With the rapid advent of atomic collision dynamics studies in highly charged heavy ions, however, an unexpectedly large contribution of the Breit interaction has been found in atomic collision processes, such as dielectronic recombination [22–27], electron-impact ionization [28], electron-impact excitation [29–31], resonant transfer and excitation [32], transfer ionization [33], and electron-electron scatterings [34]. However, even in previous experiments where strong Breit effects have been clearly demonstrated, the retardation effect therein has yet to be resolved due to experimental difficulties [22,24–30,32].

In contrast to previous atomic collision dynamics studies, the Breit effect can hardly be expected to have a significant contribution to radiative transition probabilities. For a radiative transition from the level $|a\rangle$ to $|b\rangle$, the transition rate is determined by the transition frequency ω and the transition matrix element $\langle b|\hat{\delta}|a\rangle$, where $\hat{\delta}$ represents the operator for the radiative transition. The Breit effect has no contribution to the operator $\hat{\delta}$ and only a small contribution to ω and the wave functions of $|a\rangle$ and $|b\rangle$. Consequently, transition rates are expected to be less affected by the Breit interaction. It was only found in very rare cases where the transition rates are very low (usually lower than 10^3 s^{-1}) and hence are sensitive to subtle changes in the wave function and transition frequency [35–39]. Nevertheless, we recently predicted a large modification by the Breit interaction for electric-dipole ($E1$)-allowed transitions of inner-shell excited states in highly charged heavy ions [40].

In this Letter, we report on observations of the $1s-2p$ transitions from the $1s2s^22p^2$ inner-shell excited state in boronlike

*huzhimin@scu.edu.cn

†keyao@fudan.edu.cn

‡xgao@csrc.ac.cn

W (tungsten, atomic number $Z = 74$) and Bi (bismuth, $Z = 83$) ions produced by the dielectronic capture (DC) process in an electron beam ion trap (EBIT). The high rates of $E1$ -allowed transitions ($\sim 10^{16} \text{ s}^{-1}$) are shown to be substantially modified by the Breit interaction. We elucidate that the underlying mechanism is due to the drastic change in the wave functions of the $1s2s^22p^2$ state resulting from the relativistic electron correlation effect that appeared as a Breit-interaction-induced avoided crossing. The most distinguished feature of this mechanism compared to previous experimentally studied ones is that the Breit-interaction effects in the previously studied atomic system mainly came from a single pair of electron configurations [22,24–30,32,41], whereas those in the present mechanism are determined by the ratio of two pairs of configurations. As the Breit interaction in the two pairs of electron configurations may be very different, this mechanism can greatly increase the experimental exploration range of the Breit interaction. For the present boronlike system, it turns out that the unique physical property of the two correlating energy levels composing the avoided crossing allows us to resolve the retardation effect in the electron-electron interaction experimentally. In particular, it was found that the transition rate ratio between the two $1s\text{-}2p$ transitions is affected by the retardation effect up to more than 100%.

In the present experiments, the Shanghai-EBIT [42] and the Tokyo-EBIT [43] were used for W and Bi, respectively. The volatile organic compound $\text{W}(\text{CO})_6$ was used for W injection into the trap region of the Shanghai-EBIT, and an effusion cell [44] was used for Bi injection into the Tokyo-EBIT. The operation parameters, such as beam current and trapping potential, were optimized to obtain the maximum fraction of berylliumlike ions in the trap region. To produce inner-shell excited states of boronlike ions, the electron beam energy was swept over the resonance energy region for the $KL_{12}L_3$ DC into berylliumlike ions. KLL denotes the process where the incident electron is captured into the L shell while the K shell bound electron is excited to the L shell. L_{12} and L_3 denote the orbitals with $j = 1/2$ ($2s_{1/2}$ or $2p_{1/2}$) and that with $j = 3/2$ ($2p_{3/2}$), respectively. X-ray photons emitted from the decay of the inner-shell excited states were detected by an ORTEC high-purity germanium detector placed in the direction perpendicular to the electron beam. The x-ray energy and the electron beam energy were simultaneously registered by a multichannel event-mode data acquisition system that was triggered by each x-ray photon.

The recorded two-dimensional (2D) x-ray spectra are shown in Fig. 1. On the quasidiagonal lines arising from radiative recombination (RR), x-ray enhancement due to DC followed by x-ray emission [i.e., dielectronic recombination (DR)] was observed at four main electron resonance energies for both W and Bi. Two of them (denoted as B_1 and B_2) at the lower-energy side correspond to DR forming boronlike from berylliumlike ions, and the other two (C_1 and C_2) at the higher-energy side correspond to DR forming carbonlike from boronlike ions as indicated in the figure. The intermediate inner-shell excited state for B_1 has a total angular momentum of $J = 5/2$, and can be well described by a single jj -coupled configuration state $[(1s2s^22p_{1/2})_12p_{3/2}]_{5/2}$. On the other hand, the intermediate state for B_2 has $J = 3/2$, and it can be predominantly represented as a linear combination

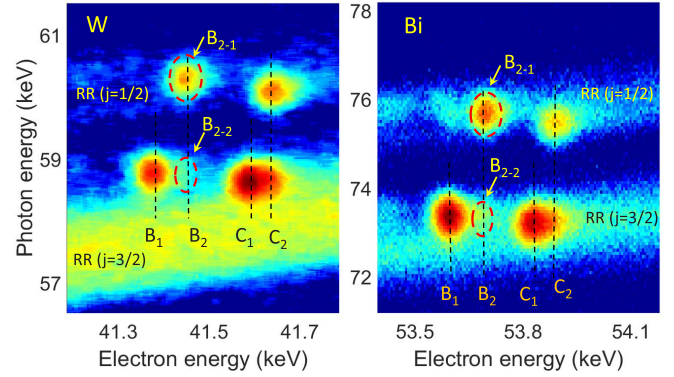


FIG. 1. Two-dimensional plots of the x-ray spectra obtained as a function of electron energy in the $KL_{12}L_3$ DR region (left for W and right for Bi). X-ray counts are plotted as a brightness of color. Bright spots correspond to x-ray enhancement due to DR.

of the two jj -coupled configurations with $J = 3/2$, which are $[(1s2s^22p_{1/2})_02p_{3/2}]_{3/2}$ and $[(1s2s^22p_{1/2})_12p_{3/2}]_{3/2}$. There are thus two states arising from the linear combination as follows (note that the common $2s^2$ closed shell is omitted in the state label),

$$|+\rangle = c_1|(1s2p_{1/2})_02p_{3/2}\rangle + c_2|(1s2p_{1/2})_12p_{3/2}\rangle, \quad (1)$$

$$|-\rangle = c_2|(1s2p_{1/2})_02p_{3/2}\rangle - c_1|(1s2p_{1/2})_12p_{3/2}\rangle, \quad (2)$$

where c_1 and c_2 are the mixing coefficients that satisfy $c_1^2 + c_2^2 = 1$, with the phase convention $c_1, c_2 > 0$. In the atomic number (Z) region of present interest, these two jj -coupled configurations strongly interact through the off-diagonal element of the Hamiltonian. According to our previous analysis [40], the intermediate state of the B_2 resonance in our experiment corresponds to $|+\rangle$ only.

Here, we investigate the radiative decay process of the level $|+\rangle$. It has two $E1$ -allowed decay paths to $1s^22s^22p_{1/2}$ (transition 1) and $1s^22s^22p_{3/2}$ (transition 2), which correspond to B_{2-1} and B_{2-2} in Fig. 1, respectively. As confirmed in Fig. 1, the x-ray intensity of transition 1 (B_{2-1}) is much stronger than that of transition 2 (B_{2-2}). To obtain an experimental x-ray intensity, DR resonance profiles were fitted to the electron energy dependence of the x-ray counts obtained by projecting the 2D plot in Fig. 1 onto the electron beam energy axis as shown in Fig. 2. The neighboring DR forming berylliumlike and carbonlike ions were also included in the fitting procedure. Fano profile functions were used for the fitting as strong quantum interference between DR and RR is known to exist in these resonances [45,46]. Since the experimental x-ray intensity I is determined by $nA W(90^\circ)$ [with n the population of the upper level, A the transition rate, and $W(\theta)$ the angular distribution factor], the radiative transition rate ratio $R = A_1/A_2$ between transitions 1 and 2, which have identical upper levels, can be obtained by

$$R = \frac{I_{B_{2-1}} W_{B_{2-2}}(90^\circ)}{I_{B_{2-2}} W_{B_{2-1}}(90^\circ)}. \quad (3)$$

The ratios determined from the experimental intensity are listed in Table I and plotted in Fig. 3(a). Angular distribution

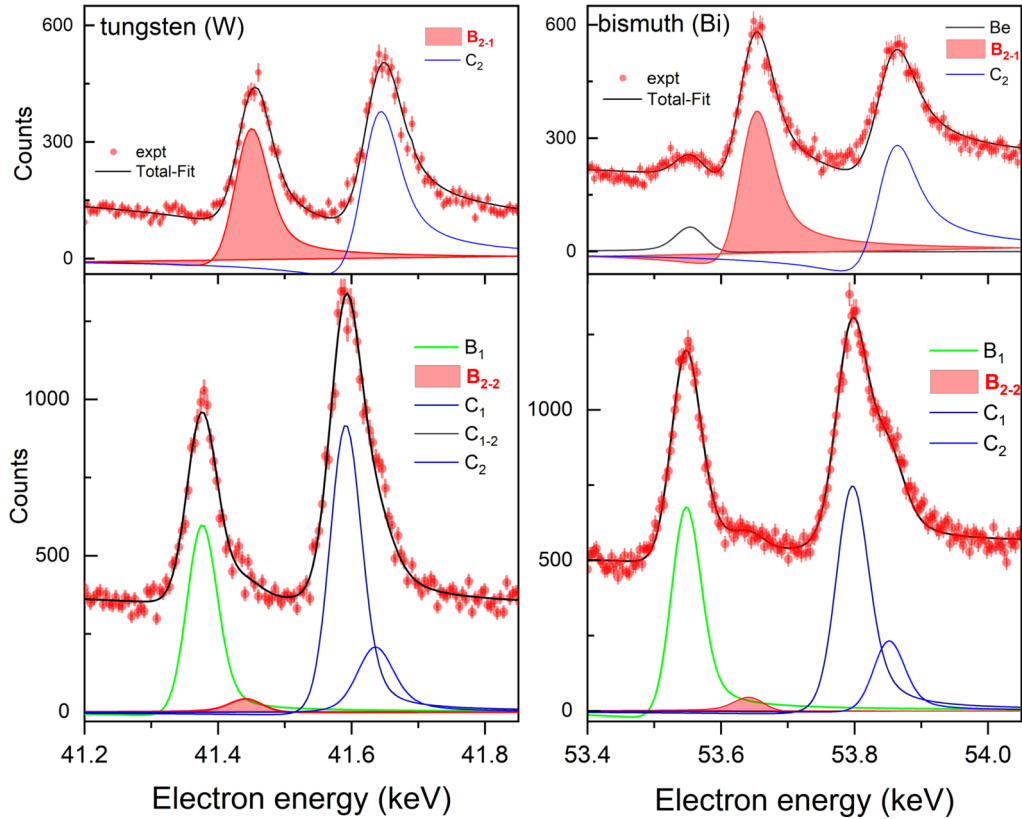


FIG. 2. Projected x-ray counts in the two RR regions: $j = 1/2$ (upper) and $j = 3/2$ (lower) (left for W and right for Bi). Red circles represent the observed x-ray counts as a function of electron energy. Solid lines represent the DR resonance profiles fitted to the observed x-ray counts.

factors calculated by the relativistic configuration-interaction approach [47] were used to obtain the ratios.

For comparison, theoretical calculations of radiative transition rates were carried out by using relativistic wave functions obtained in the multiconfiguration Dirac-Fock approach [40,48]. Figure 3 shows the results of four sets of calculations using different electron-electron interaction potentials: (i) Coulomb only; (ii) Coulomb+Gaunt interaction (only magnetic current-current terms considered in BI); (iii) Coulomb+BI with zero-frequency limit ($\omega = 0$,

TABLE I. Rates for the radiative transitions from the $|+\rangle$ level defined in Eq. (1) to $1s^22s^22p_{1/2}$ (A_1) and $1s^22s^22p_{3/2}$ (A_2), and their ratio $R = A_1/A_2$. The superscripts “th” and “expt” denote the theoretical and experimental values, respectively. Three theoretical values are obtained by including (i) the Coulomb interaction only, (ii) the Coulomb and the Gaunt, and (iv) the Coulomb and the GBI.

		A^{th} (10^{16} s^{-1})			R^{th}			R^{expt}
		(i)	(ii)	(iv)	(i)	(ii)	(iv)	
W	A_1	2.0	1.8	1.8	2.5	6.0	4.7	5.1 ± 1.3
	A_2	0.81	0.30	0.38				
Bi	A_1	3.0	2.5	2.5	2.3	8.6	5.7	5.8 ± 1.2
	A_2	1.3	0.29	0.43				

BI0) [49]; and (iv) Coulomb+generalized Breit interaction ($\omega \neq 0$, GBI), where ω is the frequency of the virtual photon exchanged between interacting electrons. The GBI includes the full retardation in the magnetic interaction as well as in the Coulomb interaction, and is identical to the Møller interaction [50–52], which was developed to describe a relativistic invariance interaction form for free electron-electron scattering. The calculated transition rates and ratios for (i), (ii), and (iv) are also listed in Table I. As shown in Fig. 3(a), the transition rate ratio monotonically decreases as Z increases when only the Coulomb interaction is considered in the electron-electron interaction potential. On the other hand, the ratios obtained by including the BI (BI is used as a generic term of BI0 and GBI hereafter) show completely different behaviors, which reproduce the experimental results quite well. This is due to the strong BI effect on the transition rates, especially on the rate A_2 of transition 2. As shown in Table I, compared with the results without including the BI, a decrease by a factor of two and three is found in A_2 for W and Bi, respectively. It should also be noted in Fig. 3(a) that the retardation effects [i.e., the difference between (ii) and (iv)] in the radiative branching ratio is very prominent, and can be clearly resolved in the experimental data for Bi. Figure 3(b) shows the Gaunt interaction (unretarded magnetic interaction) and GBI interaction (fully retarded magnetic interaction) contribute to the transition ratios with respect to the electrostatic Coulomb interaction. The contribution difference due to the retardation effect is up to more than 100%. This giant contribution of the

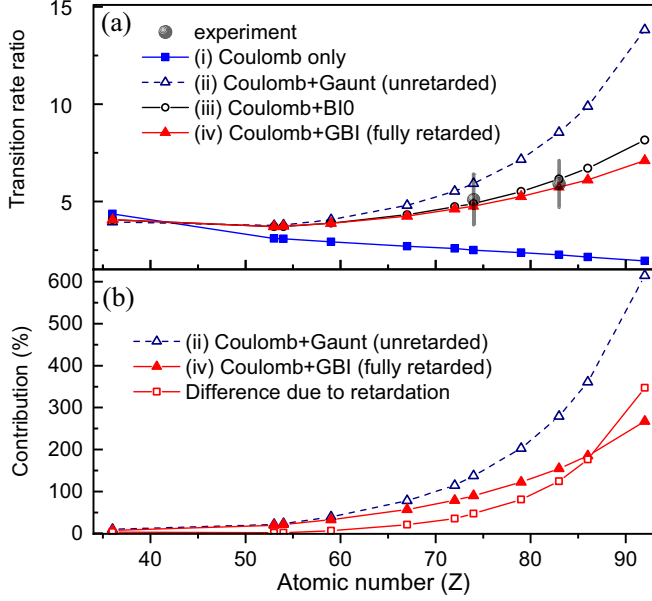


FIG. 3. (a) Transition rate ratio between two radiative transition paths of the $|+\rangle$ level. The black circles represent the experimental results. The other four symbols with solid or dashed lines are the results of four sets of calculations (see text for details). (b) Retardation-induced difference (open squares) of the contributions to the radiative transition ratios.

retardation interaction has yet to be found in electromagnetic systems, such as highly charged ions (HCIs). The underlying mechanism of the retardation effect will be discussed later.

To elucidate the underlying mechanism that realizes this strong modification on the radiative transition rates due to the BI, the energies of the $|+\rangle$ and $|-\rangle$ levels and the mixing coefficients c_1 and c_2 are plotted in Figs. 4(a) and 4(b), respectively. From the comparison between the upper and lower

panels of Fig. 4(a), the BI is found to have little effect on the energies of the $|+\rangle$ and $|-\rangle$ levels, which is as small as on the order of 0.01% or less. This is consistent with the general understanding that the energy levels are little affected by the BI. However, the mixing coefficients are greatly modified by the BI as shown in Fig. 4(b). When the BI is not considered, the coefficient c_2 is always larger than c_1 , i.e., the main jj -coupled component of the $|+\rangle$ level is $|(1s2p_{1/2})_1 2p_{3/2}\rangle$ over a whole range of Z , as shown in Fig. 4. However, when the BI is considered, the magnitude between the coefficients c_1 and c_2 is inverted at $Z = 54$ and c_1 dominates over c_2 at higher Z . Thus the nature of the $|+\rangle$ wave function drastically changes from a $|(1s2p_{1/2})_1 2p_{3/2}\rangle$ -like to a $|(1s2p_{1/2})_0 2p_{3/2}\rangle$ -like wave function as Z increases due to the BI effect. It can be shown that the jj -coupled $[(1s2s^2 2p_{1/2})_1 2p_{3/2}]_{J=3/2}$ configuration can decay both to $1s^2 2s^2 2p_{1/2}$ and $1s^2 2s^2 2p_{3/2}$, whereas $[(1s2s^2 2p_{1/2})_0 2p_{3/2}]_{J=3/2}$ can decay only to $1s^2 2s^2 2p_{1/2}$. Consequently, the ratio of transition 1 to transition 2 increases with Z in the decay of the $|+\rangle$ level.

As shown in the bottom panel of Fig. 4(a), the single configuration energies of $|(1s2p_{1/2})_0 2p_{3/2}\rangle$ and $|(1s2p_{1/2})_1 2p_{3/2}\rangle$ (E_1 and E_2), which are determined by the diagonal element of the Hamiltonian, are close to each other but never cross when the BI is not considered. Thus the $|+\rangle$ and $|-\rangle$ levels are avoided through the strong mixing arising from the off-diagonal element of the Hamiltonian but the nature of the wave function is not changed over the Z range shown in the figure, as confirmed by the almost flat dependence of the mixing coefficients on Z [open symbols in Fig. 4(b)]. On the other hand, the BI induces crossing between the single configuration energies (i.e., the diagonal Hamiltonian matrix elements) as confirmed in the upper panel of Fig. 4(a), which results in the avoided crossing between the $|+\rangle$ and $|-\rangle$ levels strongly coupled through the off-diagonal elements. This Breit-interaction-induced avoided crossing is responsible for the drastic change in the wave function before and after the crossing, and thus for the significant modification of the radiative transition rates observed in the present experiments.

The avoided crossings that appeared in the Z dependence of the energy levels were also studied previously [53,54], where the crossings realized by the change in the energy level ordering due to the coupling scheme change from LS to jj were discussed. Thus the level crossing mechanism in those studies is essentially different from that in the present study. In addition, it is worth emphasizing that the most distinguished difference is in the role of the electron-electron interaction. In the previously studied systems [53,54], the electron correlation effect can be viewed as a perturbation, and the most prominent effects appear only in the Z region near the level crossings. On the other hand, the presently studied ions belong to a strongly correlated system, where the effects last over a whole range of Z shown in Fig. 4. As the intrashell electron correlations could be important in many HCIs [55,56], the present study should have great implications in HCI-related applications.

Let us proceed to discuss the giant retardation effects observed in our system due to the avoided crossing. According to our theoretical analysis of this correlating two-level system [40], the radiative transition rate ratio is determined by the quantity Δ/V where $\Delta = E_1 - E_2$ is the energy

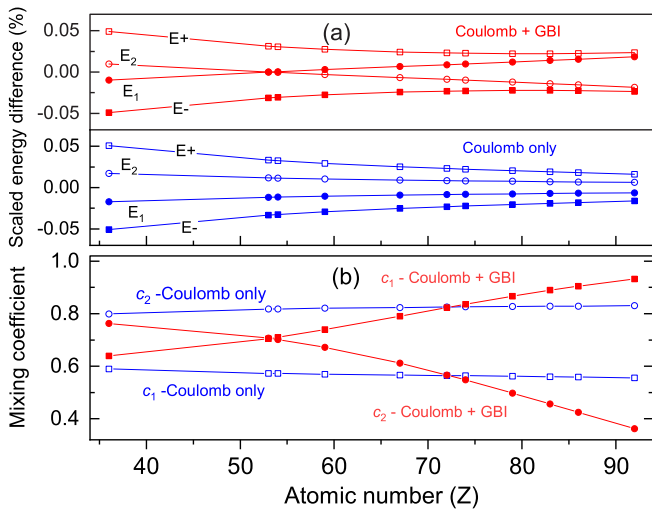


FIG. 4. (a) Scaled energy difference defined by $(E - E_{av})/E_{av}$, where E_{av} is the averaged energy of the $|+\rangle$ and $|-\rangle$ levels. E_+ and E_- represent the energy of the $|+\rangle$ and $|-\rangle$ levels, respectively. E_1 and E_2 represent the energy of the jj -coupled configurations [see Eqs. (1) and (2)]. (b) Mixing coefficients defined in Eqs. (1) and (2).

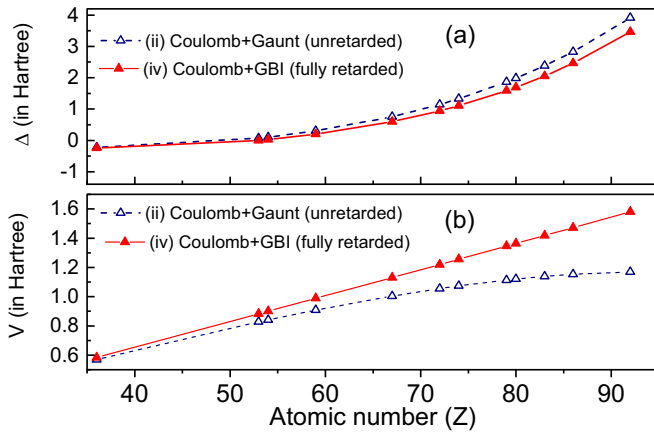


FIG. 5. (a) The energy difference of the diagonal Hamiltonian matrix elements $\Delta = E_1 - E_2$, with the two configurations defined in Fig. 4. (b) The off-diagonal Hamiltonian matrix element V between these two configurations.

difference of the diagonal Hamiltonian matrix elements and V is the off-diagonal Hamiltonian matrix element, which causes avoided crossing. In contrast to previously studied atomic systems where the Breit-interaction effects mainly came from a single pair of electron configurations [22,24–30,32,41], here the configuration pairs in Δ and V are different. As the Breit-interaction effects in the two pairs of electron configurations may be very different, this may bring in different possibilities of the Breit-interaction manifestations. For the present boron-like system, according to our numerical studies (Table S2 of Supplemental Material [48]), the Breit interaction in Δ mainly came from the electron-electron interactions between the $1s-2p_{1/2}$ orbitals, where the unretarded magnetic (Gaunt) interaction is dominant. On the other hand, the one in V mainly came from the $1s-2p_{3/2}$ orbitals where the retardation effects and Gaunt interaction are almost the same. This is caused by the fact that the direct and exchange contributions to the unretarded magnetic (Gaunt) interaction in the off-diagonal matrix element V accidentally and substantially cancel out [48].

Figures 5(a) and 5(b) show the Δ and V values, respectively. As seen in the figure, the relative contribution of the retardation effects in V is much larger than that in Δ . Since the Δ/V value is sensitive to the variation of the denominator V , the retardation effects on the radiative transition rate ratio are very prominent as shown in Fig. 3 due to the large contribution of the retardation effects on the off-diagonal matrix element V .

In summary, the electric-dipole-allowed radiative decays from the $1s2s^22p^2$ inner-shell excited state of boronlike heavy ions have been studied, and a strong Breit effect on the radiative transition rates has been shown. In particular, the giant retardation effects, which are the most crucial relativistic effects in the Breit interaction, have been clearly resolved. It is noted that the $1s-2p$ transition in lithiumlike ions exhibits completely the same physics because it has essentially the same electronic configuration as that in boronlike ions with only a difference in the existence of closed $2s^2$ electrons [40]. In addition, it can be shown that the $1s^22s^22p^2-1s2s^22p^3$ transition in carbonlike ions and the $1s^22s^22p^3-1s2s^22p^4$ transition in nitrogenlike ions are also largely modified due to the same mechanism, i.e., the Breit-interaction-induced avoided crossing [48].

We would like to acknowledge Professor Tu-Nan Chang at the University of Southern California for helpful discussions. This work was supported by the National Nature Science Foundation of China (Grants No. 12074352 and No. 11675158), the Fundamental Research Funds for the Central Universities in China (Grant No. YJ202144), and the CAEP foundation (Grants No. CX2019022 and No. YZJLX2017010). X.G. is thankful for the support by the National Natural Science Foundation of China (Grants No. 11774023 and No. U1930402), the National Key Research and Development Program of China (Grant No. 2016YFA0302104), and the National High-Tech ICF Committee in China. K.Y. is thankful for the support by the National Natural Science Foundation of China (Grant No. 11874008) and the National Key Research and Development Program of China under Grant No. 2017YFA0402300.

- [1] A. Hartung, S. Eckart, S. Brennecke, J. Rist, D. Trabert, K. Fehre, M. Richter, H. Sann, S. Zeller, K. Henrichs, G. Kastirke, J. Hoehl, A. Kalinin, M. S. Schöffler, T. Jahnke, L. P. H. Schmidt, M. Lein, M. Kunitski, and R. Dörner, Magnetic fields alter strong-field ionization, *Nat. Phys.* **15**, 1222 (2019).
- [2] N. Haram, I. Ivanov, H. Xu, K. T. Kim, A. Atia-tul Noor, U. S. Sainadh, R. D. Glover, D. Chetty, I. V. Litvinyuk, and R. T. Sang, Relativistic Nondipole Effects in Strong-Field Atomic Ionization at Moderate Intensities, *Phys. Rev. Lett.* **123**, 093201 (2019).
- [3] S. Grundmann, F. Trinter, A. W. Bray, S. Eckart, J. Rist, G. Kastirke, D. Metz, S. Klumpp, J. Viefhaus, L. P. H. Schmidt, J. B. Williams, R. Dörner, T. Jahnke, M. S. Schöffler, and A. S. Kheifets, Separating Dipole and Quadrupole Contributions to Single-Photon Double Ionization, *Phys. Rev. Lett.* **121**, 173003 (2018).
- [4] S.-G. Chen, W.-C. Jiang, S. Grundmann, F. Trinter, M. S. Schöffler, T. Jahnke, R. Dörner, H. Liang, M.-X. Wang, L.-Y. Peng, and Q. Gong, Photon Momentum Transfer in Single-Photon Double Ionization of Helium, *Phys. Rev. Lett.* **124**, 043201 (2020).
- [5] A. Ludwig, J. Maurer, B. W. Mayer, C. R. Phillips, L. Gallmann, and U. Keller, Breakdown of the Dipole Approximation in Strong-Field Ionization, *Phys. Rev. Lett.* **113**, 243001 (2014).
- [6] B. Krässig, J.-C. Bilheux, R. W. Dunford, D. S. Gemmell, S. Hasegawa, E. P. Kanter, S. H. Southworth, L. Young, L. A. LaJohn, and R. H. Pratt, Nondipole asymmetries of Kr $1s$ photoelectrons, *Phys. Rev. A* **67**, 022707 (2003).
- [7] H. B. G. Casimir and D. Polder, The influence of retardation on the London–van der Waals forces, *Phys. Rev.* **73**, 360 (1948).

- [8] R. L. Jaffe, Casimir effect and the quantum vacuum, *Phys. Rev. D* **72**, 021301(R) (2005).
- [9] L. M. Woods, D. A. R. Dalvit, A. Tkatchenko, P. Rodriguez-Lopez, A. W. Rodriguez, and R. Podgornik, Materials perspective on Casimir and van der Waals interactions, *Rev. Mod. Phys.* **88**, 045003 (2016).
- [10] D. A. T. Somers and J. N. Munday, Casimir-Lifshitz Torque Enhancement by Retardation and Intervening Dielectrics, *Phys. Rev. Lett.* **119**, 183001 (2017).
- [11] D. A. T. Somers, J. L. Garrett, K. J. Palm, and J. N. Munday, Measurement of the Casimir torque, *Nature (London)* **564**, 386 (2018).
- [12] R. Zhao, L. Li, S. Yang, W. Bao, Y. Xia, P. Ashby, Y. Wang, and X. Zhang, Stable Casimir equilibria and quantum trapping, *Science* **364**, 984 (2019).
- [13] G. Breit, The effect of retardation on the interaction of two electrons, *Phys. Rev.* **34**, 553 (1929).
- [14] G. Breit, The fine structure of He as a test of the spin interactions of two electrons, *Phys. Rev.* **36**, 383 (1930).
- [15] H. Bethe and E. Fermi, Über die wechselwirkung von zwei elektronen, *Z. Phys.* **77**, 296 (1932).
- [16] A. I. Akhiezer and V. B. Berestetskii, *Quantum Electrodynamics* (Wiley, New York, 1965).
- [17] I. P. Grant, *Relativistic Quantum Theory of Atoms and Molecules* (Springer, New York, 2006).
- [18] J. A. Gaunt, The triplets of helium, *Proc. R. Soc. London, Ser. A* **122**, 513 (1929).
- [19] J. B. Mann and W. R. Johnson, Breit interaction in multielectron atoms, *Phys. Rev. A* **4**, 41 (1971).
- [20] M. H. Chen, K. T. Cheng, and W. R. Johnson, Relativistic configuration-interaction calculations of $n = 2$ triplet states of heliumlike ions, *Phys. Rev. A* **47**, 3692 (1993).
- [21] K. T. Cheng, M. H. Chen, W. R. Johnson, and J. Sapirstein, Relativistic configuration-interaction calculations for the ground state and $n = 2$ singlet states of heliumlike ions, *Phys. Rev. A* **50**, 247 (1994).
- [22] N. Nakamura, A. P. Kavanagh, H. Watanabe, H. A. Sakaue, Y. Li, D. Kato, F. J. Currell, and S. Ohtani, Evidence for Strong Breit Interaction in Dielectronic Recombination of Highly Charged Heavy Ions, *Phys. Rev. Lett.* **100**, 073203 (2008).
- [23] S. Fritzsche, A. Surzhykov, and T. Stöhlker, Dominance of the Breit Interaction in the X-Ray Emission of Highly Charged Ions Following Dielectronic Recombination, *Phys. Rev. Lett.* **103**, 113001 (2009).
- [24] Z. Hu, X. Han, Y. Li, D. Kato, X. Tong, and N. Nakamura, Experimental Demonstration of the Breit Interaction which Dominates the Angular Distribution of X-Ray Emission in Dielectronic Recombination, *Phys. Rev. Lett.* **108**, 073002 (2012).
- [25] H. Jörg, Z. Hu, H. Bekker, M. A. Blessenohl, D. Hollain, S. Fritzsche, A. Surzhykov, J. R. Crespo Lopez-Urrutia, and S. Tashenov, Linear polarization of x-ray transitions due to dielectronic recombination in highly charged ions, *Phys. Rev. A* **91**, 042705 (2015).
- [26] C. Shah, H. Jörg, S. Bernitt, S. Dobrodey, R. Steinbruegge, C. Beilmann, P. Amaro, Z. Hu, S. Weber, S. Fritzsche, A. Surzhykov, J. R. Crespo Lopez-Urrutia, and S. Tashenov, Polarization measurement of dielectronic recombination transitions in highly charged krypton ions, *Phys. Rev. A* **92**, 042702 (2015).
- [27] D. Bernhardt, C. Brandau, Z. Harman, C. Kozhuharov, A. Müller, W. Scheid, S. Schippers, E. W. Schmidt, D. Yu, A. N. Artemyev, I. I. Tupitsyn, S. Böhm, F. Bosch, F. J. Currell, B. Franzke, A. Gumberidze, J. Jacobi, P. H. Mokler, F. Nolden, U. Spillman, Z. Stachura, M. Steck, and T. Stöhlker, Breit interaction in dielectronic recombination of hydrogenlike uranium, *Phys. Rev. A* **83**, 020701(R) (2011).
- [28] R. E. Marrs, S. R. Elliott, and J. H. Scofield, Measurement of electron-impact ionization cross sections for hydrogenlike high-Z ions, *Phys. Rev. A* **56**, 1338 (1997).
- [29] A. Gumberidze, D. B. Thorn, C. J. Fontes, B. Najjari, H. L. Zhang, A. Surzhykov, A. Voitkiv, S. Fritzsche, D. Banas, H. Beyer, W. Chen, R. D. DuBois, S. Geyer, R. E. Grisenti, S. Hagmann, M. Hegewald, S. Hess, C. Kozhuharov, R. Maertin, I. Orban, N. Petridis, R. Reuschl, A. Simon, U. Spillmann, M. Trassinelli, S. Trotsenko, G. Weber, D. F. A. Winters, N. Winters, D. Yu, and T. Stöhlker, Electron- and Proton-Impact Excitation of Hydrogenlike Uranium in Relativistic Collisions, *Phys. Rev. Lett.* **110**, 213201 (2013).
- [30] A. Gumberidze, D. B. Thorn, A. Surzhykov, C. J. Fontes, B. Najjari, A. Voitkiv, S. Fritzsche, D. Banaś, H. F. Beyer, W. Chen, R. E. Grisenti, S. Hagmann, R. Hess, P.-M. Hillenbrand, P. Indelicato, C. Kozhuharov, M. Lestinsky, R. Martin, N. Petridis, R. V. Popov, R. Schuch, U. Spillmann, S. Tashenov, S. Trotsenko, A. Warczak, G. Weber, W. Wen, D. F. A. Winters, N. Winters, Z. Yin, and T. Stöhlker, Electron- and proton-impact excitation of heliumlike uranium in relativistic collisions, *Phys. Rev. A* **99**, 032706 (2019).
- [31] C. J. Bostock, D. V. Fursa, and I. Bray, Nonperturbative electron-ion-scattering theory incorporating the Möller interaction, *Phys. Rev. A* **86**, 042709 (2012).
- [32] X. Ma, P. H. Mokler, F. Bosch, A. Gumberidze, C. Kozhuharov, D. Liesen, D. Sierpowski, Z. Stachura, T. Stöhlker, and A. Warczak, Electron-electron interaction studied in strong central fields by resonant transfer and excitation with H-like U ions, *Phys. Rev. A* **68**, 042712 (2003).
- [33] O. Y. Andreev, E. A. Mistonova, and A. B. Voitkiv, Relativistic Transfer Ionization and the Breit Interaction, *Phys. Rev. Lett.* **112**, 103202 (2014).
- [34] S. R. Greig, J. B. Khurgin, and A. Y. Elezzabi, Nonrelativistic electron-electron Møller scattering in a nonadiabatic tunnel-ionizing surface plasmon field, *Commun. Phys.* **3**, 28 (2020).
- [35] J. Doerfert, E. Träbert, A. Wolf, D. Schwalm, and O. Uwira, Precision Measurement of the Electric Dipole Intercombination Rate in C^{2+} , *Phys. Rev. Lett.* **78**, 4355 (1997).
- [36] M. H. Chen, K. T. Cheng, and W. R. Johnson, Large-scale relativistic configuration-interaction calculation of the $2s^2\ ^1S_0 - 2s2p\ ^3P_1$ intercombination transition in C III, *Phys. Rev. A* **64**, 042507 (2001).
- [37] A. Lapiere, U. D. Jentschura, J. R. Crespo López-Urrutia, J. Braun, G. Brenner, H. Bruhns, D. Fischer, A. J. González Martínez, Z. Harman, W. R. Johnson, C. H. Keitel, V. Mironov, C. J. Osborne, G. Sikler, R. Soria Orts, V. Shabaev, H. Tawara, I. I. Tupitsyn, J. Ullrich, and A. Volotka, Relativistic Electron Correlation, Quantum Electrodynamics, and the Lifetime of the $1s^2 2s^2 2p\ ^2P_{3/2}$ Level in Boronlike Argon, *Phys. Rev. Lett.* **95**, 183001 (2005).
- [38] T. R. Verhey, B. P. Das, and W. F. Perger, Multiconfiguration Dirac-Fock calculation of the forbidden $^2P_{1/2}$ to $^2P_{3/2}$ ground-state M1 transition in the boron isoelectronic sequence, *J. Phys. B: At., Mol. Opt. Phys.* **20**, 3639 (1987).

- [39] X. Y. Han, X. Gao, D. L. Zeng, J. Yan, and J. M. Li, Ratio of forbidden transition rates in the ground-state configuration of O *ii*, *Phys. Rev. A* **85**, 062506 (2012).
- [40] C. Wu, L.-Y. Xie, Z. Hu, and X. Gao, Prominent enhancement on the radiative branching ratio of the doubly excited resonant states due to the Breit interaction induced ion-core energy inversion, *J. Quant. Spectrosc. Radiat. Transfer* **246**, 106912 (2020).
- [41] R. E. Marrs, S. R. Elliott, and D. A. Knapp, Production and Trapping of Hydrogenlike and Bare Uranium Ions in an Electron Beam Ion Trap, *Phys. Rev. Lett.* **72**, 4082 (1994).
- [42] D. Lu, Y. Yang, J. Xiao, Y. Shen, Y. Fu, B. Wei, K. Yao, R. Hutton, and Y. Zou, Upgrade of the electron beam ion trap in Shanghai, *Rev. Sci. Instrum.* **85**, 093301 (2014).
- [43] N. Nakamura, J. Asada, F. J. Currell, T. Fukami, T. Hirayama, K. Motohashi, T. Nagata, E. Nojikawa, S. Ohtani, K. Okazaki, M. Sakurai, H. Shiraiishi, S. Tsurubuchi, and H. Watanabe, An overview of the Tokyo electron beam ion trap, *Phys. Scr.*, **T 73**, 362 (1997).
- [44] C. Yamada, K. Nagata, N. Nakamura, S. Ohtani, S. Takahashi, T. Tobiyama, M. Tona, H. Watanabe, N. Yoshiyasu, M. Sakurai, A. P. Kavanagh, and F. J. Currell, Injection of metallic elements into an electron-beam ion trap using a Knudsen cell, *Rev. Sci. Instrum.* **77**, 066110 (2006).
- [45] A. J. González Martínez, J. R. Crespo López-Urrutia, J. Braun, G. Brenner, H. Bruhns, A. Lapierre, V. Mironov, R. Soria Orts, H. Tawara, M. Trinczek, J. Ullrich, and J. H. Scofield, State-Selective Quantum Interference Observed in the Recombination of Highly Charged Hg^{75+...78+} Mercury Ions in an Electron Beam Ion Trap, *Phys. Rev. Lett.* **94**, 203201 (2005).
- [46] B. Tu, J. Xiao, K. Yao, Y. Shen, Y. Yang, D. Lu, W. X. Li, M. L. Qiu, X. Wang, C. Y. Chen, Y. Fu, B. Wei, C. Zheng, L. Y. Huang, B. H. Zhang, Y. J. Tang, R. Hutton, and Y. Zou, Quantum interference between resonant and nonresonant photorecombination, *Phys. Rev. A* **93**, 032707 (2016).
- [47] B. Tu, J. Xiao, Y. Shen, Y. Yang, D. Lu, T. H. Xu, W. X. Li, C. Y. Chen, Y. Fu, B. Wei, C. Zheng, L. Y. Huang, R. Hutton, X. Wang, K. Yao, Y. Zou, B. H. Zhang, and Y. J. Tang, KLL dielectronic recombination resonant strengths of He-like up to O-like tungsten ions, *Phys. Plasmas* **23**, 053301 (2016).
- [48] See Supplemental Material at <http://link.aps.org/supplemental/10.1103/PhysRevA.105.L030801> for theoretical details of the Breit interaction calculations.
- [49] Note that in fact the leading-order (in ω^2/c^2) retardation effect in the Coulomb interaction is included in BIO (see details in Sec. S1 of Supplemental Material [48]).
- [50] C. Møller, Über den stoß zweier teilchen unter berücksichtigung der retardation der kräfte, *Z. Phys.* **70**, 786 (1931).
- [51] J. Hata and I. P. Grant, Comments on relativistic two-body interaction in atoms, *J. Phys. B: At. Mol. Phys.* **17**, L107 (1984).
- [52] I. Lindgren, Gauge dependence of interelectronic potentials, *J. Phys. B: At., Mol. Opt. Phys.* **23**, 1085 (1990).
- [53] N. Nakamura, D. Kato, and S. Ohtani, Evidence for strong configuration mixing in $n = 3$ excited levels in neonlike ions, *Phys. Rev. A* **61**, 052510 (2000).
- [54] P. Beiersdorfer, J. H. Scofield, G. V. Brown, M. H. Chen, N. Hell, A. L. Osterheld, D. A. Vogel, and K. L. Wong, Avoided level crossings in very highly charged ions, *Phys. Rev. A* **93**, 051403(R) (2016).
- [55] M. Schnell, G. Gwinner, N. R. Badnell, M. E. Bannister, S. Böhm, J. Colgan, S. Kieslich, S. D. Loch, D. Mitnik, A. Müller, M. S. Pindzola, S. Schippers, D. Schwalm, W. Shi, A. Wolf, and S.-G. Zhou, Observation of Trielectronic Recombination in Be-Like Cl Ions, *Phys. Rev. Lett.* **91**, 043001 (2003).
- [56] L.-J. Dou, R. Jin, R. Sun, L.-Y. Xie, Z.-K. Huang, J.-M. Li, X.-W. Ma, and X. Gao, Relativistic eigenchannel *R*-matrix studies of the strong intrashell electron correlations in highly charged Ar¹³⁺ ions, *Phys. Rev. A* **101**, 032508 (2020).